PHYSICAL REVIEW A **66**, 013405 (2002)

Electric-field-induced relativistic Larmor-frequency reduction

P. Krekora, Q. Su, and R. Grobe
Intense Laser Physics Theory Unit and Department of Physics, Illinois State University, Normal, Illinois 61790-4560
(Received 11 February 2002; published 18 July 2002)

Using the numerical solution to the time-dependent Dirac equation we show that the effect of relativity on the usual Larmor period for an electron in a magnetic field can be enhanced drastically if a suitably scaled and aligned static electric field is added to the interaction. This electric field does not change the electron's speed but leads to an elliptical spin precession due to relativity. This spin precession is accompanied by a position-dependent spin distribution.

DOI: 10.1103/PhysRevA.66.0134XX PACS number(s): 32.80.Rm

I. INTRODUCTION

Relativistic effects have traditionally been investigated in atomic physics with respect to their impact on corrections to energy levels and transition matrix elements. Due to the availability of laser sources with very high intensity [1], recent interest has grown to also investigate those relativistic effects that arise due to the large speed atomic electrons can gain in such laser fields [2–4]. The theoretical analysis of relativistic phenomena in quantum systems relies on solutions to the Dirac equation for which analytical and nonperturbative approaches are very difficult to obtain. However, originally started in computations for heavy-ion collisions [5–7], numerical techniques to the time-dependent Dirac equation for simplified situations have been developed [8–18]. These numerical solutions are quite beneficial and have opened the door to explorations of dynamic relativistic phenomena in quantum-mechanical systems. In this work we study the effect of relativity on the time evolution of the spin for an electron wave packet in static magnetic and electric fields.

In previous works we have simulated on a computer an electron that is accelerated in a static electric field and observed that the spin component that is perpendicular to the velocity is reduced. This contraction is different compared to the usual length Lorentz contraction, which occurs in the direction parallel to the velocity. As a consequence of this kinetic relativistic mechanism the perpendicular spin component in the front of the wave packet is smaller than the component associated with the slower trailing end, as spatially resolved spin distributions for a single quantum state have revealed [14,15]. We should note that for this situation the external field does not couple directly to the spin, and due to the kinematic (which means reversible) character of this effect, the spin returns to is original value when the electron comes back to rest.

A nonkinematic and irreversible relativistic effect, however, can be observed for the same setup in the time evolution of the spatial width of the wave packet. It turns out that the spreading rate of the wave packet can be severely reduced if the wave packet attains a relativistic velocity. Due to the intrinsic coupling of the three spatial dimensions, even the spreading rate along the two spatial directions that are perpendicular to the propagation direction is suppressed. This relativistic effect first introduced in [16–18] is associated with a relativistic reduction of the velocity dispersion and leads to a spatially narrower electron wave packet even after the electron has been decelerated back to rest.

In addition to these spin and spatial contraction phenomena the time dilation effect can be observed for an electron that is injected into a static magnetic field. The center of the wave packet performs the well-known circular motion on a time scale given by the relativistic cyclotron period. Under the assumption that we can neglect effects that are exclusively associated with negative-energy states such as the *Zitterbewegung*, one finds that the product of the spin and the velocity operator is a constant of motion. In other words, the angle between the spin and the velocity remains constant. As a result, the spin performs a precession motion around the magnetic-field lines with the same Larmor period. The component of the spin that is parallel to the magnetic field remains constant at its Lorentz contracted value, whereas the other component rotates around a circle. The radius of the circle depends on the projection of the initial spin onto the initial velocity: if the projection is zero the Larmor radius is $1/(2\gamma)$ (in atomic units), where γ is the (dimensionless) relativity factor defined as $\gamma \equiv 1/\sqrt{[1-(v/c)^2]}$. On the other hand if the projection is maximum, the radius is $\frac{1}{2}$ a.u.

The next question we will address is whether there are any footprints of the Lorentz contraction with regard to the spin. Does relativity induce transitions among the spin states that can be measured when the electron returns back to rest? In Fig. 1 we have sketched a possible setup for a computer simulation. An electron wave packet initially located at rest at around $x=0$ with spin value $\langle S_y(t=0)\rangle = 0.5$ a.u. is accelerated along the x direction by a constant electric field. As a consequence, the spin will be contracted to the value $\langle S_y(t$

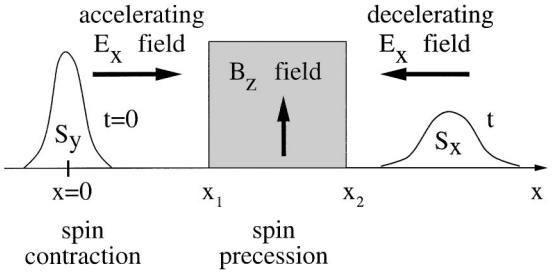

FIG. 1. Sketch of the setup permitting the observation of a relativistic spin precession motion.

$=t_1)\rangle = 1/(2\gamma)$ when it enters a zone of static magnetic field aligned along the z direction. Let us assume that the velocity of the electron has been tuned in such a way that the electron stays exactly a quarter of the Larmor period inside the magnetic-field zone. As a result, the spin initially along the y direction is rotated into the x direction. When the electron leaves the magnetic-field zone at $x=x_2$, a constant electric field decelerates the electron back to rest. The question one might ask is whether the initially contracted spin at $t=t_1$ is rotated into a spin along the x direction that is equally contracted. If this conjecture were true, the expectation value of the spin when the electron returns to rest would be smaller than 0.5 a.u., as the deceleration was along a direction parallel to the spin and therefore was not able to ''undo'' the Lorentz contraction and we would have a manifestation of an irreversible effect.

There are two levels at which this conjecture can be proven to be incorrect. The first wrong assumption is that the electron's spin would evolve along a circle. In fact, the correct spin trajectory is that of an ellipse, whose semiminor axis is perpendicular to the direction of the initial velocity and its semimajor axis is equal to $\frac{1}{2}$ a.u. In addition, the above analysis also neglected the fact that the center-of-mass motion is coupled to the magnetic field and, as a consequence, the electron would actually be rotated away from the x axis. This means that this setup in its present form is not appropriate to display the conjectured elliptical spin precession. In order to verify whether the spin precession can actually take place along an ellipse, we need to ''force'' the electron to maintain its course along the x direction. In other words, we have to couple the electron to an additional external field, which forces the electron to take a quasistraight path along the x axis.

It is the purpose of this paper to demonstrate in an *ab initio* computer simulation that an elliptical precession motion is indeed possible if we allow for an additional and suitably tuned electric field acting along the y direction, which can cancel the Lorentz force due to the magnetic field acting on the center of mass. This additional electric field couples only relativistically to the spin.

II. ELLIPTICAL SPIN PRECESSION

The interaction of a relativistic electron with an external field is described by the Dirac equation [19,20] in atomic units,

$$i\partial\Psi/\partial t = -ic\,\boldsymbol{\alpha}\cdot\boldsymbol{\nabla}\Psi + \boldsymbol{\alpha}\cdot\mathbf{A}\Psi + c^2\beta\Psi, \tag{2.1}$$

where $\boldsymbol{\alpha}$, β are the usual Dirac matrices. The vector potential $\mathbf{A}(\mathbf{r},t)$ is the sum of two parts, one modeling the static electric field with amplitude E_y along the y direction, and the other part corresponding to the static homogeneous magnetic field of strength B_z along the z direction:

$$\mathbf{A}(\mathbf{r},t) = cE_y t\mathbf{e}_y + B_z x\mathbf{e}_y. \tag{2.2}$$

The initial state is a Gaussian,

$$\Psi(\mathbf{r},t=0) = N\exp[-(x-x_0)^2/(4\Delta x^2) - (y-y_0)^2/(4\Delta y^2) - (z-z_0)^2/(4\Delta z^2)]\exp(i\mathbf{k}_0\cdot\mathbf{r})\psi(\mathbf{k}_0), \tag{2.3}$$

which has a velocity v_x along the x direction to represent the state after its acceleration at $x=x_1$ with the momentum vector $\mathbf{k}_0 \equiv \gamma v_x \mathbf{e}_x$. The spinor $\Psi(\mathbf{k}_0)$ has been chosen to be $[1,1,ck_0/(E_0+2c^2),ck_0/(E_0+2c^2)]/2$ or $[1,i,ick_0/(E_0+2c^2),ck_0/(E_0+2c^2)]/2$ to represent a spin state aligned along the x or y direction, respectively, and N is the normalization factor, with $E_0 \equiv \sqrt{c^4+c^2k_0^2}-c^2$. In a previous work [10] we have described the details of the computer algorithm that permits us to solve the time-dependent Dirac equation on a space-time grid. This algorithm is based on a split-operator scheme that requires a repeated application of the fast Fourier transformation to the Dirac state. We should mention that in order to obtain sufficiently accurate and converged data, the spatial x and y axes had to be discretized into 1024×256 intervals and the time step for the temporal advancement of the Dirac equation required up to 360 000 steps per Larmor period.

As mentioned in the Introduction, the center-of-mass motion of the electron wave packet can be effectively ''decoupled'' from the interaction with the magnetic field if the strength and alignment of the static electric field is chosen appropriately with respect to the initial velocity. In fact, for a classical point particle with an initial velocity v_x along the x direction, an electric field along the y direction, and amplitude $E_y = v_x\,\Omega$ will exactly cancel the Lorentz force associated with the magnetic field B_z along the z direction, where $\Omega \equiv B_z/c$. As a result, a point particle would travel with a constant speed along the x direction. This arrangement is used in the Wien filter for beam alignment to control and select particles that have a certain speed to charge ratio.

How good is this scheme to force an extended quantum wave packet along a straight path? The Heisenberg uncertainty in the velocity of the wave packet is approximately given by $\Delta v = 1/(2\Delta x)$; in other words, a typical range of the velocity components of the wave packet is $[-\Delta v + v_x, \Delta v + v_x]$. The interaction time with the magnetic field is on the order of the Larmor time $T_r = 2\pi\gamma/\Omega$. The time which a point particle with velocity $\Delta v + v_x$ would require to perform a full precession in the presence of the E_y field can be estimated as $2\pi c/(\Omega\Delta v)$. In other words, if the velocity width is small enough and the wave packet is sufficiently monoenergetic, the deviation of the straight line motion is negligible for the time scales considered here.

Let us now present our results. The initial velocity v_x at $x=x_1$ was chosen to be equal to $v_x = 54.8$ a.u. corresponding to 40% of the speed of light and a value of the relativity factor $\gamma \equiv 1/\sqrt{[1-(v/c)^2]} = 1.1918$, the scaled magnetic field $\Omega = 10$ a.u., and $E_y = 548$ a.u. For simplicity, we start here with an initially noncontracted spin aligned along the x direction.

In Fig. 2 we present the time evolution of the expectation value of the spin variable $\langle\mathbf{S}\rangle$ obtained from the time-dependent wave function, $\langle\mathbf{S}\rangle \equiv \langle\Psi(\mathbf{r},t)|\mathbf{S}|\Psi(\mathbf{r},t)\rangle$, where $\mathbf{S} \equiv (S_x,S_y,S_z)$ represents the three 4×4 spin matrices, and the scalar product $\langle\cdots|\cdots\rangle$ involves the spatial integration as

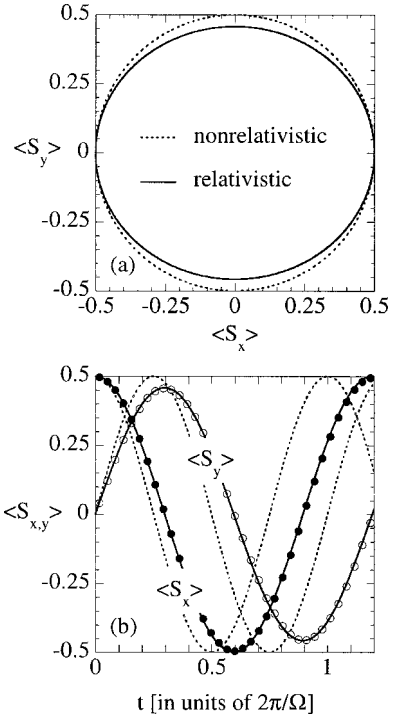

FIG. 2. The time evolution of the average spin $\langle \mathbf{S} \rangle$ (in atomic units) for a relativistic electron in combined electric and magnetic fields. (a) Parametric plot in the (S_x, S_y) plane. (b) S_x, S_y as functions of time. The dashed lines present the prediction of the nonrelativistic dynamics. The dots and circles are the numerical solutions to the time-dependent Dirac equation. The analytical formula (2.7) matches the numerical data well ($\Delta x = \Delta y = 1$ a.u., $v_x = 54.9$ a.u., $v_y = 0$, $\Omega = 10$ a.u., and $E_y = 548$ a.u.).

well as the summation of the four spinor components. Figure 2(a) shows the dynamics in the (S_x, S_y) plane. The ellipse is apparent, its semiminor axis is 0.457 a.u., which agrees within 0.25% to the value of $1/(2\gamma) = 0.458$ a.u. For comparison, the dashed line in the figure represents the usual nonrelativistic circular precession motion. The time evolution of the spin is resolved in Fig. 2(b). The period of the motion can be directly taken from the graph as 0.7511 a.u., which agrees with the numerical value of $T \equiv 2\pi\gamma^2/\Omega$ up to an error of only 0.75%. This period exceeds the nonrelativistic Larmor period $2\pi/\Omega$ by 19.1%, and it is 9.5% larger than the relativistic Larmor period $2\pi\gamma/\Omega$ for the circular precession.

Some approximate but analytical estimates for the amplitude as well as the unusual period can be derived if we transform our coordinate system into the rest frame with regard to the center of mass. The transformation of the lab electric and magnetic field into the effective ones for the rest frame yield, in general [21],

$$\mathbf{E}_r = \gamma(\mathbf{E} - \boldsymbol{\beta} \times \mathbf{B}) - \gamma^2/(1+\gamma)\boldsymbol{\beta}(\boldsymbol{\beta} \cdot \mathbf{E}), \tag{2.4a}$$

$$\mathbf{B}_r = \gamma(\mathbf{B} + \boldsymbol{\beta} \times \mathbf{E}) - \gamma^2/(1+\gamma)\boldsymbol{\beta}(\boldsymbol{\beta} \cdot \mathbf{B}), \tag{2.4b}$$

where $\boldsymbol{\beta} = v_x/c\,\mathbf{e}_x$, $\mathbf{E} = E_y \mathbf{e}_y$ and $\mathbf{B} = B_Z \mathbf{e}_z$. Due to the specific choice of the orientation and size of the electric field ($E_y = v_x B_z/c\,\mathbf{e}_y$), the effective magnetic field in the rest frame amounts to $\mathbf{B}_r = \mathbf{B}/\gamma$, whereas $\mathbf{E}_r$ vanishes entirely. Due to the absence of the electric field in the rest frame, the dynamics of the spin operator in the rest frame time t_r can be simply obtained from the solution to

$$\frac{d}{dt_r}\mathbf{S_r} = \mathbf{S_r} \times \mathbf{B_r}/c. \tag{2.5}$$

Returning to the lab frame, the spin matrices need to be transformed with the Lorentz boost matrix L, defined as [19]

$$L = \exp[(\omega/2)\alpha_x] = \cosh\frac{\psi}{2}\begin{bmatrix} 1 & 0 & 0 & \tanh\frac{\omega}{2} \\ 0 & 1 & \tanh\frac{\omega}{2} & 0 \\ 0 & \tanh\frac{\omega}{2} & 1 & 0 \\ \tanh\frac{\omega}{2} & 0 & 0 & 1 \end{bmatrix} \tag{2.6}$$

with

$$\alpha_x \equiv \begin{bmatrix} 0 & \sigma_x \\ \sigma_x & 0 \end{bmatrix},$$

where $\sigma_x \equiv \left[\begin{smallmatrix} 0 & 1 \\ 1 & 0 \end{smallmatrix}\right]$ and $\omega \equiv a \tanh(v_x/c)$.

We transform back to the lab time according to $t = \gamma t_r$ and calculate the expectation values from the operator solution. In order to obtain simple analytical expressions we had to assume that the expectation value of the product of the spin operator and a nontrivial velocity function can be factorized. We obtain the expression for the time evolution of the elliptical spin precession:

$$\langle S_x(t) \rangle = \langle S_x(0) \rangle \cos(\Omega/\gamma^2 t) - \langle S_y(0) \rangle \sin(\Omega/\gamma^2 t)\,\gamma, \tag{2.7a}$$

$$\langle S_y(t) \rangle = \langle S_x(0) \rangle \sin(\Omega/\gamma^2 t)/\gamma + \langle S_y(0) \rangle \cos(\Omega/\gamma^2 t), \tag{2.7b}$$

$$\langle S_z(t) \rangle = \langle S_z(0) \rangle. \tag{2.7c}$$

In order to examine the validity of this approximate formula, its prediction has been superimposed on the exact numerical data obtained from the wave packet presented in Fig. 2. The simple analytical estimate seems to be quite valid for these parameters. In fact, the two corresponding graphs are practically indistinguishable for each spin component. This agreement is remarkable in view of the fact that the spatial extension and the velocity dispersion of the wave packet were neglected in the analytical derivation. We should note that, to the best of our knowledge, this is the first example of a relativistic time scale in a quantum system that depends quadratically on the velocity factor γ and not just linearly.

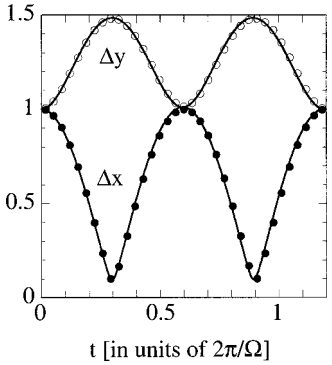

FIG. 3. The time evolution of the spatial widths Δx and Δy for a wave packet (in atomic units). The circles mark the numerical data points and solid lines present the prediction of the approximate analytical formula (3.1) (same parameters as in Fig. 2).

III. SPATIAL DENSITY DISTRIBUTION DURING THE ELLIPTICAL SPIN PRECESSION

Following the analysis of the spin dynamics, let us now investigate the space-time development of the spatial wave packet for the same setup. As discussed, despite the presence of the magnetic field, the center-of-mass motion is effectively decoupled from the field and the wave packet evolves with a constant speed. The spatial width of the packet, however, shows some interesting features that we will analyze next. In Fig. 3 we display the time dependence of the widths of the wave packet $\Delta x(t) \equiv \sqrt{[\langle x^2\rangle - \langle x\rangle^2]}$ and $\Delta y(t)$ during the first cycle. The expected wave packet spreading is completely suppressed and replaced by a nearly periodic time evolution. After $\frac{1}{4}$ of the relativistic Larmor period the initially spherical wave packet has deformed into a cigar shaped distribution, the width Δx along the propagation direction is reduced by almost 90%, whereas the transverse width Δy has grown from its initial value $\Delta y(t=0)=1$ to 1.48 a.u. This periodic breathing pattern [22] is reminiscent of the way the electron was originally introduced into the magnetic field. The response of a spatially extended wave packet to a static magnetic field depends on whether the electron travels into the magnetic field or whether the magnetic field was turned on as a function of time. In either case the electron experiences in its rest frame a short electric field which can affect its motion. Due to the gauge choice of the vector potential $\mathbf{A}=B_z x \mathbf{e}_y$ in Eq. (2.2), the magnetic field turn-on effect is associated with an electric-field pulse which can instantly alter the velocity distribution of the wave packet. In fact, the corresponding electric-field δ pulse creates a strongly correlated dependence of the velocity component and the respective position. The initial velocity along the x direction is unaffected, as the x component of the E-field pulse is zero; however, the velocity along the y direction is changed by the x-position-dependent amount Ωx. In other words, electrons within the wave packet that are located at the positive x axis have the amount $v_y(t=0)=\Omega x$ added to their original value that is associated with the Heisenberg uncertainty. For weak magnetic fields this additional boost velocity is negligible, however, for the size of the magnetic fields discussed in our situation, this effect can be quite important. As the result of these strongly position correlated velocities the dynamics of the wave-packet width shows the breathing patterns displayed in Fig. 3.

Following a similar procedure which led to Eq. (2.7) above, one can also derive some approximate analytical expressions for these breathing patterns by first analyzing the effect in the electron's rest frame using the effective fields of Eq. (2.4). Again, neglecting any impact of the negative-energy eigenstates, the Heisenberg equations of motion for the position operator can be solved for an electron in the effective magnetic field. This solution can be used to approximate the time evolution of the spatial variance in our quantum state. If we Lorentz transform the results back into the lab frame we obtain

$$\begin{aligned}
\Delta x^2(t) &= \Delta x^2 \cos^2(\Omega/\gamma^2 t) + 1/[2\Omega^2 \Delta y^2][1-\cos(\Omega/\gamma^2 t)]^2 \\
&\quad + 1/[2\Omega^2 \Delta x^2 \gamma^2]\sin^2(\Omega/\gamma^2 t), \\
\Delta y^2(t) &= \Delta y^2 + \gamma^2 \Delta x^2 \sin^2(\Omega/\gamma^2 t) \\
&\quad + \gamma^2/[2\Omega^2 \Delta y^2]\sin^2(\Omega/\gamma^2 t) \\
&\quad + 1/[2\Omega^2 \Delta x^2][1-\cos(\Omega/\gamma^2 t)], \\
\Delta z^2(t) &= \Delta z^2. \qquad (3.1)
\end{aligned}$$

The prediction according to these equations is superimposed in Fig. 3 by the circles. The agreement is actually quite good in view of the fact that the analytical derivation was based on several approximations. A discrepancy with the exact numerical data could be associated with the approximation to use the effective fields according to Eq. (2.4) for the entire wave packet as well as the factorization assumption when computing the expectation values. The fields are only exact for the center-of-mass motion. Second, we have neglected relatively for the position operator solution in the rest frame. The latter approximation was necessary to simplify the analytical calculation of the expectation values for the variances.

Let us conclude this section with a comment about a numerical simplification with respect to the dimensionality of the problem. All aspects of the motion along the spatial z direction are basically decoupled from the dynamics, which simplifies the numerical solution of the Dirac equation significantly. On the other hand, our numerical simulations indicate that a further reduction of the dynamics to only one spatial dimension (x direction) has almost no impact on the (three-dimensional) spin data $\langle \mathbf{S}(t)\rangle$ presented in Fig. 2, and even the graph for $\Delta x(t)$ shown in Fig. 3 is very closely reproduced by a one-dimensional calculation. If one is only interested in the spatial variable along the x direction, this feature can lead to significant numerical reduction in CPU time. In fact, the data presented in Fig. 3 took 40 CPU days on an Origin 2000 cluster of supercomputers for the simulation in all dimensions.

IV. SPATIAL SPIN DISTRIBUTION

Interesting relativistic effects can also be observed in the spatial spin distribution. In previous works [14,15] we have

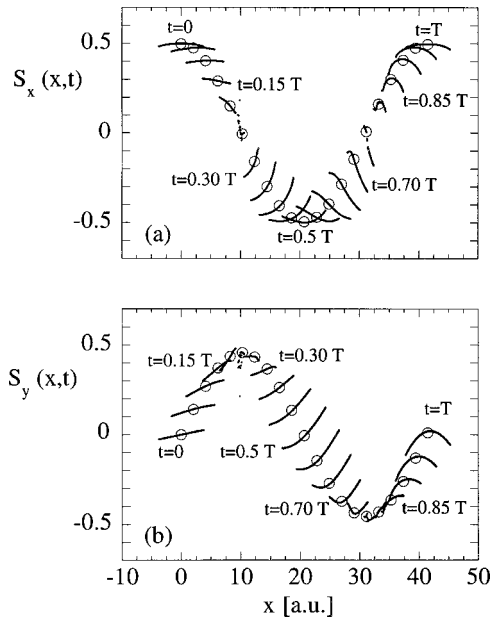

FIG. 4. Snapshots of the spatial spin densities $S_x(x,t)$ and $S_y(x,t)$ of the electron's wave packet (in atomic units) as it travels along the x axis for times that are $\frac{1}{20}$ of the relativistic Larmor period T apart (same parameters as in Fig. 2).

defined a position-dependent spin density, which allows one to distinguish between different values of the spin within a single quantum state. These densities can be defined as

$$\mathbf{S}(\mathbf{r},t)\equiv\Psi^{\dagger}(\mathbf{r},t)\mathbf{S}\Psi(\mathbf{r},t)/[\Psi^{\dagger}(\mathbf{r},t)\Psi(\mathbf{r},t)], \qquad (4.1)$$

where $\mathbf{S}\equiv(S_x,S_y,S_z)$ consists of the usual 4×4 spin matrices. $\mathbf{S}(\mathbf{r},t)$ is the average value of the spin one would measure if the electron were detected at time t and location $\mathbf{r}$. Please note that the reference to the word ''average'' is used in a quantum statistical sense; any individual measurement, of course, leads to $\pm\frac{1}{2}$ a.u. From this definition it follows that $\langle\mathbf{S}(t)\rangle=\langle\Psi^{\dagger}(\mathbf{r},t)|\mathbf{S}|\Psi(\mathbf{r},t)\rangle=\int d\mathbf{r}\,\mathbf{S}(\mathbf{r},t)\mathbf{P}(\mathbf{r},t)$, where $\mathbf{P}(\mathbf{r},t)\equiv\Psi^{\dagger}(\mathbf{r},t)\Psi(\mathbf{r},t)$ is the spatial probability density, given by the sum of the four squared spinor components of the wave function. In the absence of any relativistic effects, the spin density would remain position independent in a spatially homogeneous magnetic field.

In Fig. 4 we show the corresponding spin densities at various times for our case. As the wave packet moves along the x axis, we display the values of the spin density only over a spatial region of total length $4\Delta x(t)$ that is centered at the position of the packet at that time. To better guide the eye, the circles displayed in the figure represent the expectation values of the spin as shown in Fig. 2.

The spin density of the initial state is nearly flat. In other words, one would measure the same spin value independent of the position of the detector. The minor corrections to a perfectly flat distribution are associated with the fact that it is not possible for a spatially finite wave packet to be in an exact spin eigenstate.

The development of the spin density into one with a nonuniform distribution can be understood qualitatively. As an example, after a time of $t=0.15T$ the front portion of the wave packet has a lower spin value $\langle S_x\rangle$ as the trailing edge. In the discussion in Sec. III we have seen that due to the magnetic-field turn-on effect, the initial wave packet has position-dependent velocities along the y direction each of which leads to a circular motion in the rest frame. After a short time this effect leads to a reduced (increased) speed v_x of the front (trailing) part of the wave packet. This effect leads to an effectively less contracted magnetic field for the front than for the back, and the spin component S_x in the front requires a shorter Larmor period than the trailing part at that instant in time. As a result, the front spin evolves ahead of the back spin and the density $S_x(x,t)$ monotonically decreases with x. The same argument explains why the density for $S_y(x,t)$ is tilted in the other direction at that time. It might be interesting to note that both spin distributions $S_x(x,t)$ and $S_y(x,t)$ do not return to their precise initial distribution after a Larmor period. This is expected because even the time evolutions of the spin expectation values are not strictly periodic due to relativity for a wave packet with a finite spatial extension.

V. SUMMARY AND CONCLUSION

Using the numerical solution of the time-dependent Dirac equation for an electron in suitably tuned and aligned combined electric and magnetic fields, it is shown that the spin precession can take place along an elliptical trajectory due to relativistic effects. We derived approximate analytical expressions for the time evolution of the spin expectation value that match well with the numerical data obtained from the wave-function solution. It turns out that, due to the presence of the static electric field, the impact of relativity can be enhanced significantly. The Larmor frequency is $2\pi\gamma^2/\Omega$ and not $2\pi\gamma/\Omega$ as one could expect from a simulation of the usual circular relativistic precession motion in a magnetic field alone. In contrast to the spatial dynamics, the electric field can only partially cancel the magnetic field for the spin dynamics. This increase of the Larmor period by a factor of γ enables the measurement of relativistic effects at effectively lower electron speeds. Another relativistic effect can be observed in the position-dependent spin density, which, in contrast to the flat nonrelativistic distribution, changes its shape as a function of time in a quasiperiodic fashion.

The present work is part of a sequence of projects aimed at identifying relativistic effects in a quantum system that do not have a direct counterpart in a corresponding theory based on classical mechanics. We began this specific study with the hope of finding a suitable experimental setup in which a nonreversible effect of relativity on the spin motion could be detected. However, as it turns out, the relativistically induced spin transitions that are associated with the Lorentz contraction do not have their manifestation when the electron is decelerated back to nonrelativistic speeds. Possibly other interactions can be used to obtain a more irreversible impact of relativity on the quantum-mechanical laser-atom interaction.

ACKNOWLEDGMENTS

We thank Professor G. H. Rutherford and R. E. Wagner for several helpful discussions. This work has been supported by the NSF and Research Corporation. The numerical part of this work was performed at NCSA.

[1] For a review, see G. A. Mourou, C. P. J. Barty, and M. D. Perry, Phys. Today **51(1)**, 22 (1998).
[2] For reviews, see *Relativistic Effects in Strong Electromagnetic Fields*, edited by H. R. Reiss, special issue of Opt. Express **2**, 261 (1988).
[3] See, e.g., Q. Su and R. Grobe, in *Multiphoton Processes*, edited by L. F. DiMauro, R. R. Freeman, and K. C. Kulander, AIP Conf. Proc. No. 525 (AIP, Melville, NY, 2000), p. 655.
[4] R. E. Wagner, Q. Su, and R. Grobe, Phys. Rev. Lett. **84**, 3282 (2000).
[5] C. Bottcher and M. R. Strayer, Ann. Phys. (N.Y.) **175**, 64 (1987).
[6] J. C. Wells, A. S. Umar, V. E. Oberacker, C. Bottcher, M. R. Strayer, J.-S. Wu, J. Drake, and R. Flanery, Int. J. Mod. Phys. C **4**, 459 (1993).
[7] K. Momberger, A. Belkacem, and A. H. Sorensen, Phys. Rev. A **53**, 1605 (1996).
[8] N. J. Kylstra, A. M. Ermolaev, and C. J. Joachain, J. Phys. B **30**, L449 (1997).
[9] U. W. Rathe, C. H. Keitel, M. Protopapas, and P. L. Knight, J. Phys. B **30**, L531 (1997).
[10] J. W. Braun, Q. Su, and R. Grobe, Phys. Rev. A **59**, 604 (1999).
[11] R. E. Wagner, P. J. Peverly, Q. Su, and R. Grobe, Phys. Rev. A **61**, 035402 (2000).
[12] P. Krekora, R. E. Wagner, Q. Su, and R. Grobe, Phys. Rev. A **63**, 025404 (2001).
[13] J. S. Roman, L. Plaja, and L. Roso, Phys. Rev. A **64**, 063402 (2001).
[14] P. Krekora, Q. Su, and R. Grobe, J. Phys. B **34**, 2795 (2001).
[15] Q. Su, P. J. Peverly, R. E. Wagner, P. Krekora, and R. Grobe, Optics Express **8**, 51 (2001).
[16] Q. Su, B. A. Smetanko, and R. Grobe, Optics Express **2**, 277 (1998).
[17] Q. Su, B. A. Smetanko, and R. Grobe, Laser Phys. **8**, 93 (1998).
[18] E. Lenz, M. Doerr, and W. Sandner, in *Super-Intense Laser Physics*, edited by B. Piraux and K. Rzazewski (Kluwer Academic, Dordrecht, 2001), p. 355.
[19] J. D. Bjorken and S. D. Drell, *Relativistic Quantum Mechanics* (McGraw-Hill, New York, 1964).
[20] B. Thaller, *The Dirac Equation* (Springer, New York, 1992).
[21] J. D. Jackson, *Classical Electrodynamics*, 3rd ed. (Wiley, New York, 1998).
[22] J. C. Csesznegi, G. H. Rutherford, Q. Su, and R. Grobe, Laser Phys. **9**, 41 (1999).